Nonlocal Drift Modes in Cylindrical Geometry

Francis F. Chen

Citation: Physics of Fluids **10**, 1647 (1967); doi: 10.1063/1.1762340
View online: http://dx.doi.org/10.1063/1.1762340
View Table of Contents: http://scitation.aip.org/content/aip/journal/pof1/10/8?ver=pdfcov
Published by the AIP Publishing

Nonlocal Drift Modes in Cylindrical Geometry

FRANCIS F. CHEN
Plasma Physics Laboratory, Princeton University, Princeton, New Jersey
(Received 13 February 1967)

Numerical computations are given for resistive drift instabilities of a plasma in a conducting cylinder, for cases where the usual WKB analysis fails because the waves are not localized radially by shear in the drift velocity. The finite boundary conditions are found to have a stabilizing effect on flute modes ($k_\parallel = 0$) and a destabilizing effect on drift modes ($k_\parallel \neq 0$). The growth rate for drift waves is more than three times larger than that given by "local" dispersion relations. These computations are particularly relevant to oscillations in cesium and potassium plasmas.

IN the usual treatment of universal drift instabilities of an inhomogeneous plasma in a magnetic field,[1] the phase-integral method is employed for approximating the solution to the radial wave equation. This approximation is a good one when the radial wavenumber n is large and when there are turning points lying within the plasma, so that the waves are localized to a layer inside the plasma. In the laboratory, however, drift waves are generally found to have a weak radial dependence; and the wave amplitude satisfies the radial boundary condition not by an exponential decay towards the boundary but simply by having a node there. It is our purpose to examine the growth and propagation characteristics of such nonlocalized modes; this necessarily involves numerical solution of the wave equation.

Localization of drift modes in the usual treatments comes about because the gradient in the drift velocity $V_{de} \equiv -(kT/eB)\,(\partial \ln n/\partial r)$ is assumed to be nonvanishing.[2] Then drift waves are localized because they cannot stay in phase over a large range of radius r. However, these localized waves, which have large growth rates, can quickly wipe out the gradients in V_{de}, leaving a plasma in uniform rotation, subject only to the nonlocalized perturbations discussed here.

Consider, then, an infinitely long cylindrical plasma column rotating uniformly in a homogeneous magnetic field. If resistive excitation is dominant, the wave equation describing drift and centrifugal instabilities in such a system is that given in a previous paper[3]

$$\frac{d^2W}{dz^2} + \left[-\frac{1}{4} + \frac{1 + N(z)}{2z} + \frac{1 - m^2}{4z^2}\right]W = 0, \quad (1)$$

where

$$N(z) = \frac{\Psi(1 + 2s) + s^2 + i(\Psi - 2)y^2e^z}{\Psi(1 - \Psi)}. \quad (2)$$

Here $T_i = T_e$ has been assumed; W is the wave amplitude, varying as $\exp i(m\theta + k_\parallel\zeta - \omega t)$ in the cylindrical coordinates (r, θ, ζ); z is a radial variable $z \equiv (r/r_0)^2$, r_0 being the density-gradient scale distance; $\Psi \equiv (\omega - m\omega_0)/\omega^*$ is the frequency in the ion frame in units of the electron diamagnetic drift frequency $\omega^* \equiv (m/r)V_{de} = m\rho^2\omega_c$, where $\rho \equiv r_L/r_0$, r_L and ω_c being the ion Larmor radius and cyclotron frequency; $s \equiv m\omega_0/\omega^*$ is the "spin" of the plasma column, the ion rotation frequency in units of ω^* (note that $m\omega_0 \neq -\omega^*$ whenever the zero-order radial electric field is finite); $y \equiv (k_\parallel r_L/\rho^2)\cdot(2m\epsilon_0)^{-\frac{1}{2}}$ is a suitably normalized $k_\parallel$; and $\epsilon_0 \equiv n_0e\eta/B$ is the normalized resistivity η on the axis.

When $k_\parallel = y = 0$, $N(z)$ is independent of z; and Eq. (1) reduces to Whittaker's equation. If the radial boundary is taken at infinity, one obtains the Rosenbluth–Krall–Rostoker[4] result for gravitational flute instabilities driven by the centrifugal force

$$N\Psi^2 + (1 + 2s - N)\Psi + s^2 = 0, \quad (3)$$

where $N = 2n + m$, $n = 0, 1, 2, \cdots$ being the radial wavenumber. When $y \neq 0$, the local dispersion relation can be found by neglecting the derivative in Eq. (1) and solving numerically the resulting complex algebraic equation for Ψ. When y is sufficiently large, the wave becomes a drift wave; and the local dispersion relation can be approximated by[5]

$$\Psi = 2 + iy^{-2}e^{-z}[2(N + 1 + 2s) + s^2], \quad (4)$$

$$N = \frac{m^2 - 1}{2z} + \tfrac{1}{2}k_r^2r_0^2 + \tfrac{1}{2}z - 1, \quad (5)$$

[1] For instance, N. A. Krall and M. N. Rosenbluth, Phys. Fluids **8**, 1488 (1965).
[2] Here n is the plasma density, not to be confused with the radial wavenumber used elsewhere in this paper.
[3] F. F. Chen, Phys. Fluids **9**, 965 (1966), Eqs. (43) and (44).
[4] F. F. Chen, Phys. Fluids **9**, 965 (1966), Eq. (31); M. N. Rosenbluth, N. A. Krall, and N. Rostoker, Nucl. Fusion Suppl. Pt. 1, 143 (1962).
[5] F. F. Chen, Phys. Fluids **9**, 965 (1966), Eqs. (49) and (50).

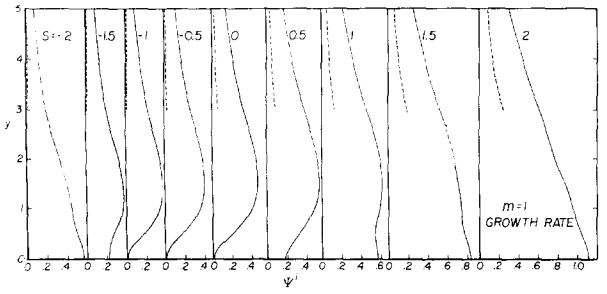

FIG. 1. The growth rate Ψ^i, in units of the drift frequency, for the $m = 1$ mode as a function of y, which is proportional to $k_\parallel$, for various values of normalized rotation frequency s. Dashed curves are the "local" approximation. The curves are computed for the lowest radial mode with the boundary at $Z = (R/r_0^2) = 2$.

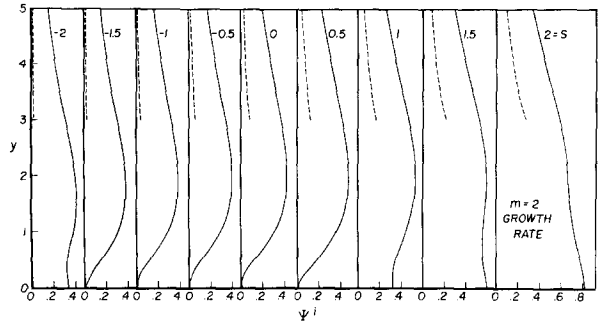

FIG. 2. Growth rate Ψ^i for the $m = 2$ mode.

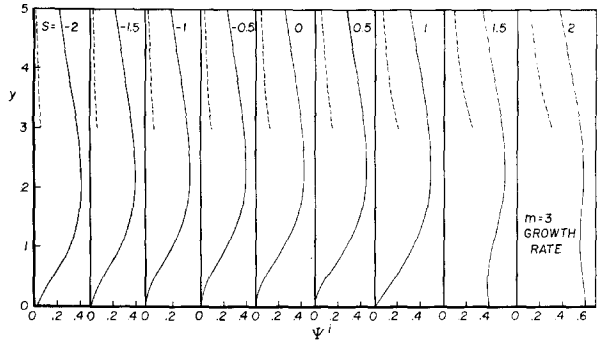

FIG. 3. Growth rate Ψ^i for the $m = 3$ mode.

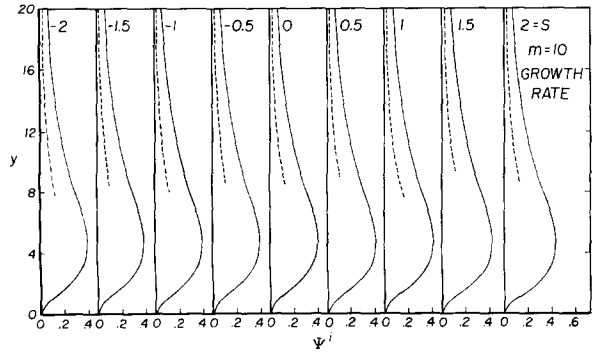

FIG. 4. Growth rate Ψ^i for the $m = 10$ mode.

where k_r is the local value of the radial component of $\mathbf{k}$. For the lowest radial mode we have set $\frac{1}{2}k_r^2 r_0^2 \approx 1$. For small values of m, however, the exact radial dependence becomes important, and Eqs. (4) and (5) cannot be expected to give accurate results.

To treat these experimentally interesting cases, we have numerically solved the differential equation (1) with the boundary condition that $W = 0$ at $r = 0$ and $r = R$. In the laboratory, the radial boundary is usually defined by a conducting annulus of internal radius R which acts as an aperture limiter. Such a limiter has a short-circuiting effect on potential fluctuations outside the aperture, and generally the level of oscillation is much lower there than inside; hence our condition $W = 0$ for $r \geq R$ is a good approximation. On the other hand, the density at $r = R$ does not have to vanish because it takes a finite time for ions which have diffused to the edge to travel along $\mathbf{B}$ to the aperture limiter, where they recombine. In the computations we have taken $Z \equiv (R/r_0)^2 = 2$ or 3, corresponding to density ratios $n(R)/n_0 = 0.135$ and 0.050, respectively. These are in the range of what is commonly found experimentally.

The results for the normalized frequency Ψ^r and growth rate Ψ^i as functions of y (normalized $k_\parallel$) for various values of m and s are presented in Figs. 1–8. To obtain a pair of eigenvalues (Ψ^r, Ψ^i), we started with a large value of y and guessed Ψ^r and Ψ^i from the local approximation, Eqs. (4) and (5). Equation (2) then gave $N(z)$. The complex equation (1) was then iterated inward from $r = R$ with initial slope -1. In general, $|W|$ would be far from zero at $r = 0$. A new trial pair (Ψ^r, Ψ^i) was then found by a method described by Fox[6] and adapted to complex eigenvalues by Goldberg, and the process was iterated until $|W|$ at $r = 0$ was less than a prescribed value. For subsequent values of y, the initial trial pair (Ψ^r, Ψ^i) was found by extrapolation from the previous three values of y. Each of the curves in Figs. 1–8 was traced from more than 20 computed points.

Also shown in Figs. 1–8 are dashed curves indicating the "local" approximation obtained from Eqs. (4) and (5). Consider first the growth rates Ψ^i shown in Figs. 1–4. The case $s = -1$ corresponds to the pure resistive drift mode with no radial electric field; the case $s = 0$ is the case of zero-mass rotation occurring when the ion diamagnetic drift is cancelled by an E/B drift. The $y = 0$ flute mode

[6] L. Fox, in *Boundary Problems in Differential Equations*, R. E. Langer, Ed. (University of Wisconsin Press, Madison, Wisconsin, 1960), p. 243.

is stable between these values of s. For $m = 1$, the flute mode becomes unstable when the rotation frequency s goes outside these limits. This is the centrifugal instability discussed in Ref. 3, where it was pointed out that the asymmetry between positive and negative values of s is due to the Coriolis force. For $m = 2$, 3, and 10, the region of stability for the flute mode progressively widens as finite Larmor radius stabilization becomes more effective. As y is increased, the growth rate reaches a maximum and then falls again as the wave becomes a drift mode at large y. In the drift region the growth rate increases as m is increased because finite Larmor radius effects excite drift oscillations rather than damp them, at least in the $k_\perp^2 r_L^2 \ll 1$ regime assumed here. It is seen that the local dispersion relation underestimates Ψ^i by at least a factor of 3 in all cases but is a better approximation for $m = 10$ than for low m, as expected. Note that all the curves for $m = 10$ are nearly identical. This is because finite Larmor radius stabilization has quenched the gravitational instabilities caused by the centrifugal force (proportional to s^2), and what is left is the universal growth rate (independent of s).

Consider now the real frequencies Ψ^r shown in Figs. 5–8. We have displaced the curves by plotting $\Psi^r + s$, which is the normalized frequency in the laboratory frame. $\Psi^r = 2$ corresponds to a wave propagating at the electron drift velocity V_{de}. The drift wave at large y approaches this value asymptotically in all cases. The flute mode at $y = 0$ always propagates in the ion drift direction in the $E = 0$ frame. This can be seen from Figs. 5–8 by realizing that Ψ^r in the $E = 0$ frame is $(\Psi^r + s) - (1 + s)$. For $m = 10$, this velocity is small, so that the curves in Fig. 8 are almost equally spaced. For $m = 1$, the flute velocity can exceed V_{di}, causing the bunching of frequencies at the bottom of Fig. 5.

Figure 9 shows the effect of the finite boundary condition on the flute modes. The solid lines are the predictions of the remote-boundary result, Eq. (3), for $n = 0$. The points are the $y = 0$ points of Figs. 1–8, computed for $Z = (R/r_0)^2 = 2$. For $m = 2$, 3, and 10, it is seen that the flute mode is made more stable by the boundary. This is in general agreement with a calculation by Lehnert[7] on this special case of $y = 0$. For $m = 1$, however, Eq. (3) predicts absolute stability, whereas the growth rate is actually larger than for $m = 2$ if the boundary is taken into account. The problem does not arise

[7] B. Lehnert, Phys. Fluids 9, 1367 (1966).

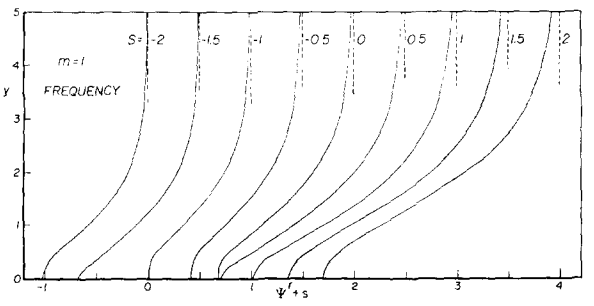

FIG. 5. The frequency $\Psi^r + s$ in the laboratory frame, in units of the drift frequency, for the $m = 1$ mode. Other notes under Fig. 1 apply.

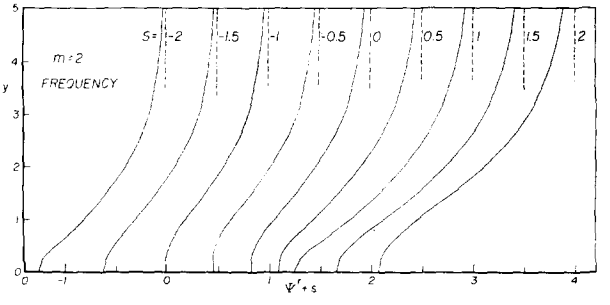

FIG. 6. Frequency $\Psi^r + s$ for the $m = 2$ mode.

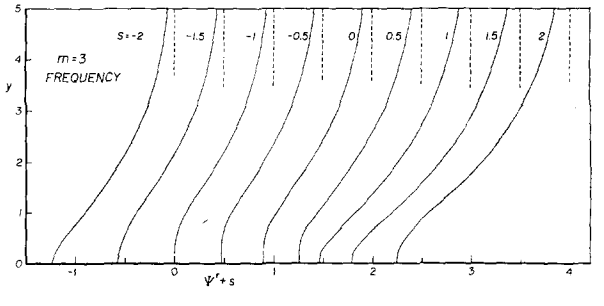

FIG. 7. Frequency $\Psi^r + s$ for the $m = 3$ mode.

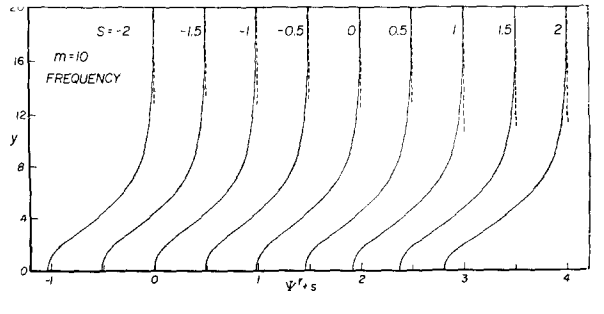

FIG. 8. Frequency $\Psi^r + s$ for the $m = 10$ mode.

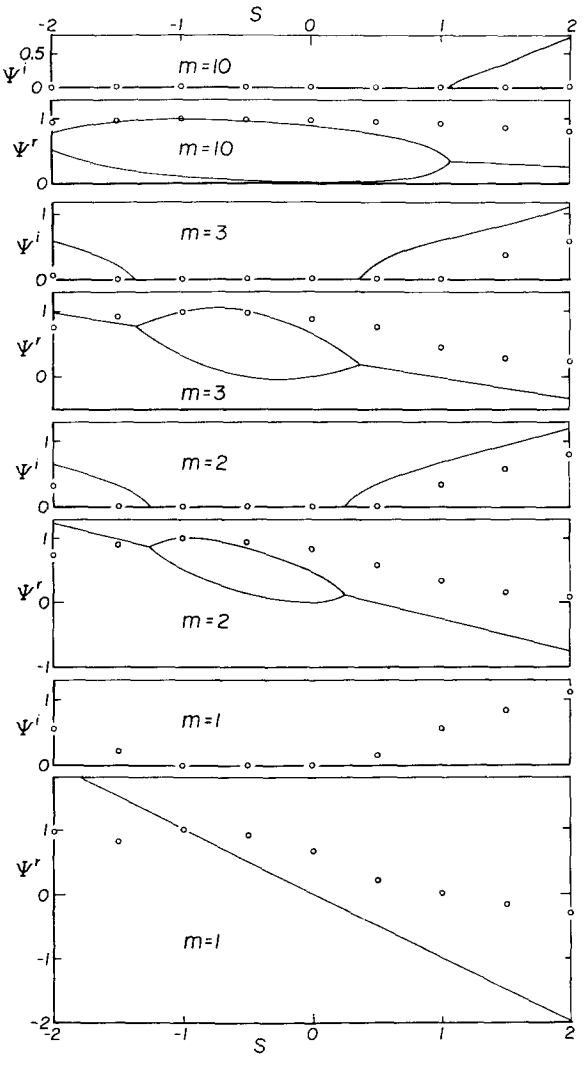

FIG. 9. Frequencies Ψ^r and growth rates Ψ^i as a function of spin s for the $m = 1, 2, 3$, and 10 modes of the centrifugal flute instability with $k_\parallel = 0$. Solid lines are from remote-boundary theory; points are finite-boundary computations.

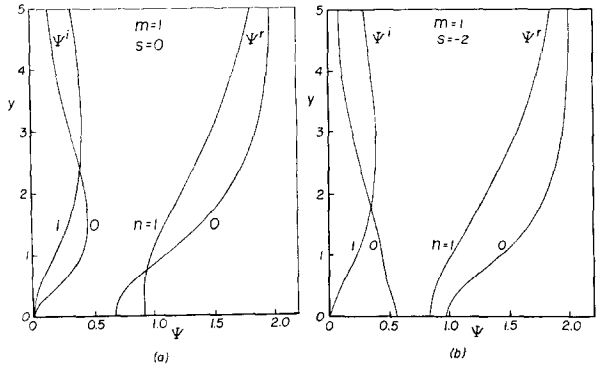

FIG. 10. Dependence of the $\Psi - y$ dispersion curves on radial mode number n, for $m = 1$ and (a) $s = 0$ and (b) $s = -2$.

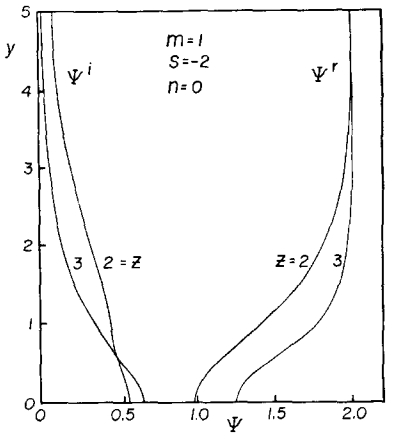

FIG. 11. Dependence of the $\Psi - y$ dispersion curves on the boundary position Z, for $m = 1$, $n = 0$, and $s = -2$.

in Lehnert's paper because plane geometry was used. This result has several experimental implications. An explanation by Rostoker and Kolb[8] for the appearance of an $m = 2$ instability in a θ-pinch, without $m = 1$, would appear to be fortuitous. Secondly, the observation of $m = 1$ oscillations in cesium plasmas does not necessarily imply a drift wave. In view of the finite-boundary result, these oscillations could also be centrifugal flute modes, and $k_\parallel$ or the velocity of propagation in the θ direction has to be measured to tell these apart.

Figure 10 shows the effect of the radial wavelength; computations for the lowest ($n = 0$) and

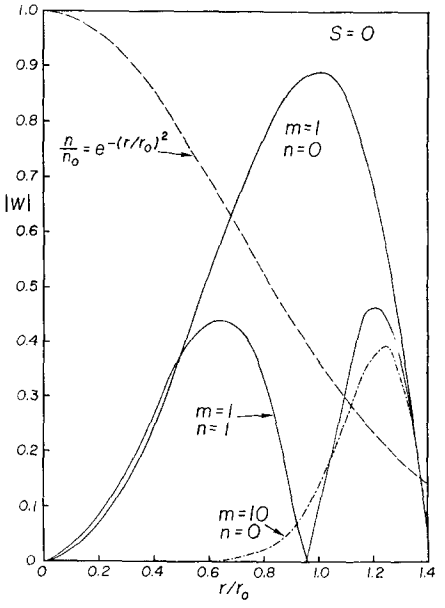

FIG. 12. Radial amplitude distribution for the $m = 1$, $n = 0$; $m = 1$, $n = 1$; and $m = 10$, $n = 0$ modes for $s = 0$. The dashed line shows the zero-order density profile.

[8] N. Rostoker and A. C. Kolb, Phys. Rev. 124, 965 (1961).

next higher ($n = 1$) radial mode are compared. Just as the finite Larmor radius effects were increased by increasing m in Figs. 1–8, the same finite Larmor radius effects come into play with increasing n. As before, we see that the flute modes ($y \approx 0$) are stabilized by finite Larmor radius effects, whereas the drift modes (large y) are destabilized by them.

Figure 11 shows the effect of changing the boundary position from $Z = 2$ to $Z = 3$. Since finite Larmor radius effects are stronger when the radial wavelength is diminished by decreasing Z, we see again that the finite Larmor radius stabilizes flute modes but destabilizes drift modes, as pointed out earlier.[9] The parameters of Fig. 6 have been chosen to be useful for experiments in Q-machines, where the radial electric field[10] corresponds to $s = -2$. Note that the frequency of the flute mode seems to be sensitive to the radial boundary conditions.

[9] F. F. Chen, Phys. Fluids **8**, 912 (1965).
[10] F. F. Chen, Phys. Fluids **9**, 2534 (1966).

In Fig. 12 we show the radial variation of amplitude for three cases. It is interesting that the radial width of the lowest radial mode for $m = 10$ is much smaller than for $m = 1$. This supports the assumption, made by many theorists on plasma turbulence, that the radial and azimuthal wavelengths are of the same order of magnitude. For the Gaussian density distribution assumed, $\nabla n/n$ is largest at the boundary; and indeed we see that the $m = 10$ peak is shifted outwards.

ACKNOWLEDGMENTS

The numerical computations for this article were made by L. Goldberg, to whom the author is profoundly grateful.

Use was made of computer facilities supported in part by National Science Foundation Grant NSF-GP 579. This work was performed under the auspices of the United States Atomic Energy Commission, Contract No. AT(30-1)-1238.